

TWO DIMENSIONAL IMPEDANCE ANALYSIS OF SEGMENTED IVU*

A. Blednykh[#], G. Bassi, J. Bengtsson, O. Chubar, C. Kitegi, T. Tanabe
BNL, Photon Sciences, Upton, New York, 11973-5000, U.S.A.

Abstract

Segmented In-Vacuum Undulator (IVU) with variable magnetic gap along z-axis is considered as an alternative to the Constant Gap IVU for the NSLS-II storage ring. The length of the Constant Gap IVU for a given minimum gap is limited by the beam stay clear aperture. With the new conceptual design of IVU the magnetic gap can be varied along z-axis and its minimum gap can be reduced up to 5.25mm for the same stay clear aperture. Beam impedance becomes an important issue since the new design consists of several magnet gaps. Wakepotentials and impedances have been analyzed for a new type of IVU and the results compared with data for the reference geometry which is the Constant Gap IVU.

INTRODUCTION

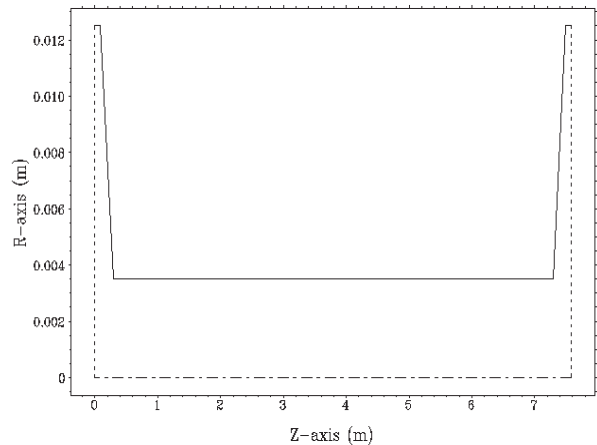
Intensive calculations of magnetic field, radiation flux and brightness for segmented adaptive-gap in-vacuum undulators is presented in work [1]. Their gain in spectral performance over standard in-vacuum undulators, both for room-temperature and cryo-cooled realizations is demonstrated. The next step is to estimate their contribution into the total impedance of the ring and compare their results with data for existing Constant Gap IVU.

We analyzed three geometries of in-vacuum undulators (IVU's), Constant Gap IVU with 7mm full gap (Fig. 1a), Stepped Gap Variation IVU (Fig. 1b) with varied gaps along z-axis and Linear Gap Variation IVU (Fig. 1c) with copper-nickel foil on top of two magnet arrays which was made by straight lines to connect steps of magnetic gaps. For numerical analysis we used the ABCI code [2] and the ECHO code [3, 4].

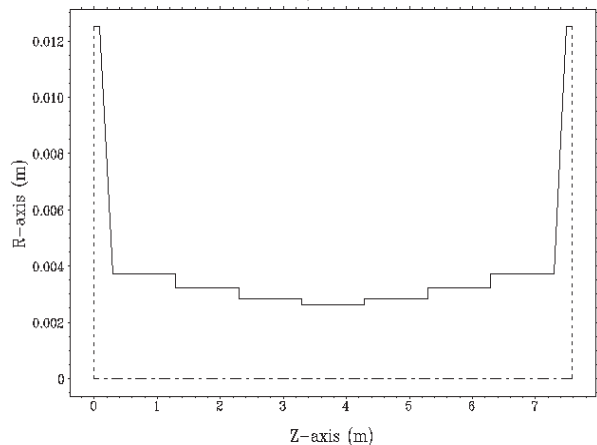
Since there is a concern that the electron bunches going through the segmented IVU (Fig. 1b and Fig. 1c) can generate much stronger short-range and long-range wakepotentials due to several steps inside we compared all our results with data for the Constant Gap IVU. The Constant Gap IVU is used as the reference geometry.

The Constant Gap IVU has a 7mm full gap. The magnetic gap of the Stepped Gap Variation IVU and the Linear Gap Variation IVU are varied from 5.25mm up to 7.5mm and its length about 1m. The full vertical aperture of the NSLS-II vacuum chamber is 25mm. The same smooth transition is applied for all three geometries and its length is $L_T = 200mm$.

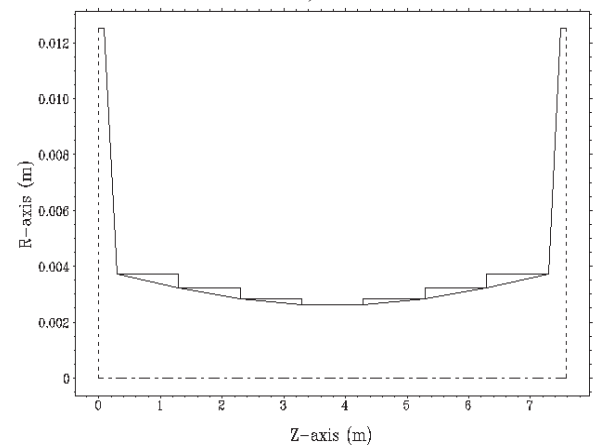
Insertion devices in the NSLS-II storage ring will be installed after the commissioning (Phase 1). During the phase commissioning no insertion devices and no Landau cavities will be installed into the ring (Bare lattice).



a)



b)



c)

Figure 1: Geometries of in-vacuum undulators. a) Constant Gap IVU with 7mm full gap. b) Stepped Gap Variation IVU with varied gaps along z-axis. The minimum full gap is 5.25mm. c) Linear Gap Variation IVU with magnetic gap edges connected by straight lines.

*Work supported by DOE contract No: DE-AC02-98CH10886

[#]blednykh@bnl.gov

Our calculations are performed for a bunch length of $\sigma_s = 4.5\text{mm}$ when damping wigglers (DW's) and insertion devices will occupy straight sections of NSLS-II (Phase 2).

We pay special attention here to heating issues due to image current and to coupled-bunch effects due to narrow-band impedance. Single bunch effects have been studied for many of the Constant Gap IVU's in [5, 6, 7]. To estimate the microwave threshold with several segmented IVU's in the ring we would need to calculate the longitudinal wakepotential for $\sigma_s = 0.05\text{mm}$ bunch length and apply this wakepotential and wakepotentials of other components as well for beam-dynamics simulations. To estimate Transverse Mode Coupling Instability (TMCI) threshold we would need to know the location of IVU's in straight section with low- β function or with high- β function and their quantity.

LONGITUDINAL IMPEDANCE

The longitudinal short-range wakepotential is shown in Fig. 2 for three different geometries. Since the magnet arrays will be covered by copper-nickel foil the Stepped Gap Variation IVU is considered as a worst case scenario. In all three cases the wakepotentials look inductive and do not differ significantly. The bunch length is $\sigma_s = 4.5\text{mm}$ and we are in the regime when $\sigma_s > b$, where b is the minimal radius of IVU.

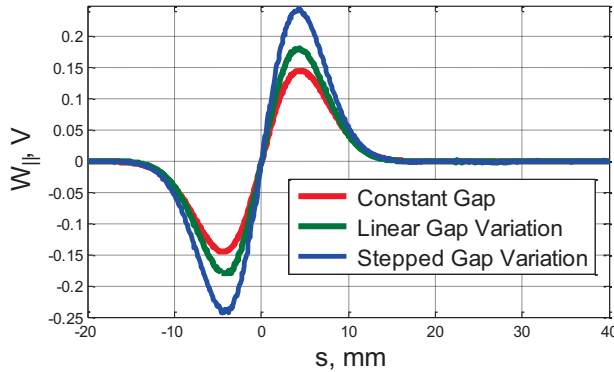


Figure 2: Longitudinal short-range wakepotential for three different geometries.

The real part of the longitudinal narrow-band impedance for the considered geometries is shown in Fig. 3. The first longitudinal lowest mode which can be generated by the beam is E_{01} -Mode with $j_{01} = 2.405$ the first root of the Bessel function. The first resonance peak is seen at frequency $f_r = 9.72\text{GHz}$ and based on calculations (Fig. 3) its frequency does not depend on the radius b . It depends on the maximal radius d . Segmented IVU's (Fig. 1b and Fig. 1c) have a minimal radius of 2.6mm . The radius of the Constant Gap IVU is 3.5mm . By varying the radius the resonance frequency is not changed. The cutoff frequency, E_{01} -Mode, of a round pipe with 12.5mm and 3.5mm radii are $f_c^{12.5\text{mm}} = 9.18\text{GHz}$ and $f_c^{3.5\text{mm}} = 32.79\text{GHz}$ respectively. The resonant mode can propagate at $f_r > f_c$.

The loss factor is shown in Table 1 for all three geometries. The geometric loss factor does not change too much since there are no big differences between the longitudinal wakepotentials and the real part of the impedances. The loss factor due to resistive wall [8] for $L=7\text{m}$ has the dominant effect for IVU geometries and it is drastically larger than the geometric loss factor. Since radii are slightly different from geometry to geometry the loss factor due to resistive wall has some small difference.

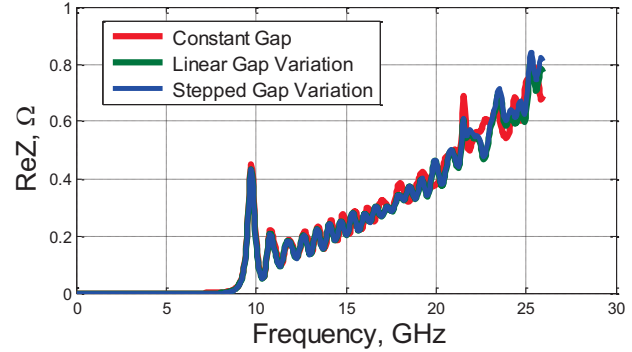


Figure 3: Real part of the longitudinal narrow-band impedance.

The power loss is presented for a case of 300mA average current in 1080 bunches. The revolution period of the NSLS-II storage ring is $2.6\mu\text{s}$. With employing Landau Cavity we would expect bunch lengthening by at least a factor of two. For $\sigma_s = 9\text{mm}$, the total loss factor ($\kappa_{loss}^{Geom.} + \kappa_{loss}^{RW}$) will drop down since it has a dependence on σ_s , but the average current will be increased up to 500mA . Taking into account these changes the power loss will remain at a level of 20W .

Table 1: Loss Factors ($\sigma_s = 4.5\text{mm}$) and Power Losses for Geometries Shown in Fig. 1

	$\kappa_{loss}^{Geom.}$ mV/pC	κ_{loss}^{RW} mV/pC	Power loss @300mA P_{loss}, W
Constant Gap, $b = 3.5\text{mm}$	0.89	108	24
Linear Gap Variation, $b_{av} = 3.2\text{mm}$	0.84	118	26
Stepped Gap Variation, $b_{av} = 3.2\text{mm}$	0.84	118	26

TRANSVERSE IMPEDANCE

Based on the transverse impedance derived by K. Yokoya for the round tapered collimator [9] we can write the transverse kick factor as

$$\kappa_{\perp} = \frac{Z_0 c}{2\pi^{3/2}} \frac{d-b}{\sigma_s L} \left(\frac{1}{b} - \frac{1}{d} \right), \quad \frac{d-b}{L} \frac{b}{\sigma_s} \ll 1 \quad (1)$$

where d is the large beam pipe radius, b is the small beam pipe radius, L is the taper length, σ_s is the bunch length, c is the velocity of light and Z_0 is the impedance of free space. For the Constant Gap IVU with $d = 12.5\text{mm}$, $b = 3.5\text{mm}$ and $L = 200\text{mm}$ (Fig. 1a) the transverse geometric kick factor due to Eq. (1) is 21V/pC/m . The numerically calculated kick factor for the same geometry (Table 2) agrees well with the kick factor obtained by Eq. (1). The transverse kick factors in Table 2 calculated for the considered geometries used the transverse wakepotentials presented in Fig. 4. The wakepotentials for the Constant Gap IVU (green curve) and for the Linear Gap Variation IVU (orange curve) are almost repeating each other and hence the kick factor for both geometries does not change too much. It can be explained by a longer smooth transition which is formed due linear connection of all steps. Since the kick factor is inversely proportional to the taper length and the taper length in the Linear Gap Variation IVU becomes significantly longer ($\sim 3\text{m}$) that compensate even the change in radius up to 2.6mm to keep the wakepotential comparable with the wakepotential for the Constant Gap IVU.

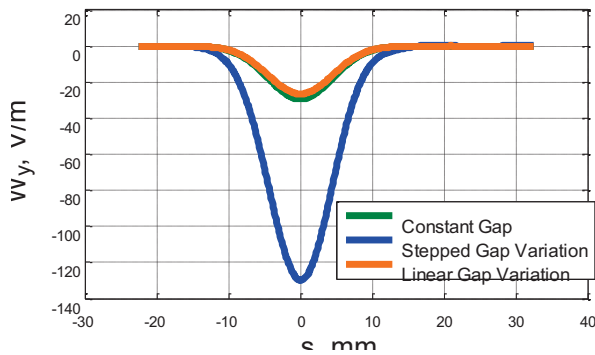


Figure 4: Vertical geometric short-range wakepotentials for three different geometries are shown in Fig. 1.

The magnitude of the wakepotential for the Stepped Gap Variation IVU (blue curve) is by a factor of ~ 4 larger to be compared with wakepotentials of other two geometries. Electromagnetic fields radiate at small steps and it affects the bunch perturbation. As a result the wakepotential for the considered structure is much stronger and the kick factor is larger (Table 2). As we discussed earlier the copper-nickel foil will be applied for IVU to minimize its contribution to the total impedance of the ring. Based on our 2D analysis the results of impedance and wakepotentials do not deviate too much for two IVU geometries, with linear gap variation and with constant gap. In the case of the Linear Gap Variation IVU, the minimal gap (5.25mm) is smaller than the gap of the Constant IVU (7mm), which is preferable for optimization of brightness and flux density.

The transverse kick factor due to resistive wall is a bit higher for the Linear Gap Variation IVU since the average radius is smaller. The resistive wall effect needs to be optimized for any IVU geometries to reduce their impact on the total impedance of the ring.

Table 2: Kick Factor for a $\sigma_s = 4.5\text{mm}$ Bunch Length

	$\kappa_{\perp}^{Geom.}$ $V/pC/m$	$\kappa_{loss}^{RW,Gap}$ $V/pC/m$	$\kappa_{loss}^{RW,Taper}$ $V/pC/m$
Constant Gap	21	263	2.5
		(Al 7m $b = 3.5\text{mm}$)	(Al 0.4m $b_{av} = 8\text{mm}$)
Linear Gap Variation	19	344	2.5
		(Al 7m $b_{av} = 3.5\text{mm}$)	(Al 0.4m $b_{av} = 8\text{mm}$)
Stepped Gap Variation	91	388	2.5
		(Al 7m Σb_i)	(Al 0.4m $b_{av} = 8\text{mm}$)

CONCLUSION

Impedance and wakepotential analysis showed that the IVU structure with linear gap variation can be integrated into the NSLS-II storage ring. The results for the IVU structure with linear gap variation do not deviate too much from the results for the IVU with the constant gap. The 3D IVU structure is going to be analysed next. The calculated wakepotentials will be implemented into the OASIS (Optimal Algorithm for Selfconsistent Instability Simulations) code [7,10] for particle-tracking simulations.

REFERENCES

- [1] O. Chubar, J. Bengtsson, A. Blednykh, C. Kitegi, T. Tanabe "Spectral Performance of Segmented Adaptive-Gap In-Vacuum Undulators for Storage Rings", IPAC'2012, current proceeding.
- [2] Yong Ho Chin, <http://abci.kek.jp/abci.htm>, ABCI code.
- [3] I. Zagorodnov and T. Weiland, Phys. Rev. ST Accel. Beams 8, 042001 (2005).
- [4] I. Zagorodnov, Phys. Rev. ST Accel. Beams 9, 102002, (2006).
- [5] A. Blednykh, S. Krinsky, B. Podobedov and J.-M. Wang, "Transverse Impedance of Small-Gap Undulators for NSLS-II", Proceeding of EPAC 2006.
- [6] A. Blednykh, S. Krinsky, B. Nash and L. Yu, "Microwave Instability Simulations for NSLS-II", Proceeding of PAC 2009.
- [7] G. Bassi and A. Blednykh, "Study of Single and Coupled-Bunch Instabilities for NSLS-II", Proceeding of PAC 2011.
- [8] K.L.F. Bane and M. Sands, "Short Range Resistive Wall Wakefields", AIP Conf. Proc. 367,131 (1995)
- [9] K. Yokoya, "Impedance of Slowly Tapered Structures", Tech. Rep. SL/90-88 (AP), CERN (1990).
- [10] G. Bassi, "OASIS, a Parallel Self-consistent Algorithm for Instability Simulations", in preparation.